JOURNAL OF INTEGRATED OMICS
A METHODOLOGICAL JOURNAL
HTTP://WWW.JIOMICS.COM

ORIGINAL ARTICLE | DOI: 10.5584/jiomics.v2i1.85

Elucidation of carbon transfer in a mixed culture of *Acidiphilium cryptum* and *Acidithiobacillus ferrooxidans* using protein-based stable isotope probing

René Kermer[1], Sabrina Hedrich[2,3], Martin Taubert[1], Sven Baumann[4], Michael Schlömann[2], D. Barrie Johnson[3], Martin von Bergen[1,4] and Jana Seifert*[1].

[1]Department of Proteomics, UFZ – Helmholtz Centre for Environmental Research, Permoserstr. 15, D-04318 Leipzig, Germany; [2]Interdisciplinary Ecological Center, TU Bergakademie Freiberg, Leipziger Strasse 29, 09599 Freiberg, Germany; [3]School of Biological Sciences, College of Natural Sciences, Bangor University, Deiniol Road, Bangor LL57 2UW, U.K.; [4]Department of Metabolomics, UFZ - Helmholtz Centre for Environmental Research, Permoserstr. 15, D-04318 Leipzig, Germany.

Received: 16 December 2011 **Accepted:** 21 February 2012 **Available Online**: 08 March 2012

ABSTRACT

Although many examples of syntrophic cultures are known, details of carbon utilization and carbon transfers within them often remain elusive due to limitations in methods used to detect carbon flux. We have applied the recently developed method of protein-based stable isotope probing (protein-SIP) to track carbon flow in a mixed culture of acidophilic bacteria. The heterotroph *Acidiphilium cryptum* was grown in the presence of ^{13}C-labeled galactose, together with the iron- and sulfur-oxidizing autotroph *Acidithiobacillus ferrooxidans*. Cultures were harvested at five time points, proteins extracted and separated by 1-dimensional SDS gel electrophoresis, peptides obtained by tryptic digest of gel slices and analyzed by UPLC Orbitrap MS/MS measurements. Syntrophic interactions were confirmed by analysis of the time-dependent incorporation of ^{13}C into peptides, and quantified by calculation of relative isotope abundance (RIA) and labeling ratio (lr) from mass spectral isotope patterns. $^{13}CO_2$ formed by catabolism of galactose by *A. cryptum*, was found to be assimilated by *At. ferrooxidans* which used tetrathionate as electron donor. Mass spectral data indicated that ^{13}C-labeled organic substances, mostly peptides, secreted by the chemoautotroph were assimilated by the heterotroph. The data provided unequivocal evidence for two-way transfer of carbon in mixed cultures of autotrophic and heterotrophic acidophilic bacteria.

Keywords: Mass spectrometry; protein-SIP; acidophiles; carbon flux.

1. Introduction

Stable isotope probing (SIP) is an emerging tool for investigating metabolic key players in microbial communities and their interaction mechanisms [1]. In brief, substrates are labeled with heavy isotopes, such as ^{13}C, ^{15}N or ^{36}S, which are then incorporated into biomolecules by the metabolic activity of the cells [2-4]. In addition to the application of SIP with nucleic acids, the use of proteins in SIP has recently been established [2, 3, 5, 6]. As proteins closely reflect the cell activity at any time point, this approach enables concomitant functional analysis of microbial communities.

In protein-SIP, the incorporation of heavy isotopes can be detected as a mass shift of peptides derived from the analyzed proteins which can be measured by mass spectrometric analysis. From a peptide mass spectrum, the quantification of the fraction of heavy isotopes of a specific element, e.g. ^{13}C, referred to as relative isotope abundance (RIA), is possible either in a sequence-dependent or sequence-independent approach, with the latter using the half decimal place rule [7-9]. For the sequence-dependent approach, an accuracy of ± 0.1% ^{13}C RIA using at least 20 peptides has been claimed [10] .

Besides the RIA data, the intensity ratio between labeled and unlabeled peptide forms is also of interest, especially in time-series experiments. This 'labeling ratio' (lr) was recently

***Corresponding author:** Jana Seifert, E-mail Address: jana.seifert@ufz.de; Phone Number: +49 341 235 1352; Fax Number: +49 341 235 1786 .

used to detect induction of specific proteins after a substrate shift based on differences in protein synthesis rates [8]. The potential of protein-SIP to detect metabolic activities in defined communities as well as in enrichment cultures was also proven in recent studies [2, 11, 12], though a demonstration of the applicability of protein-SIP to detect the carbon flux between different species has not previously been reported.

Acidithiobacillus (At.) ferrooxidans was the first acidophilic bacterium shown to oxidize ferrous iron as well as reduced sulfur and has subsequently been shown to oxidize hydrogen and formic acid. The pH range of the type strain is 1.5 to >4.0 with an optimum for growth of about 2.0 [13-16]. The genus *Acidithiobacillus* currently comprises four recognized species, two of which (*At. ferrooxidans* and the psychrotolerant species *At. ferrivorans*) are iron oxidizers [17, 18] and all of which are autotrophs. The physiological diversity and versatility of iron-oxidizing metabolic activity may be the reason for the wide distribution of this genus in a variety of acid mine drainage sites [19].

Acidiphilium spp. are obligately heterotrophic acidophiles (with the exception of *Acidiphilum (A.) acidophilum*, which is a facultative autotroph) that are widely distributed in metal-rich, acidic environments [20]. They can grow on a wide range of monosaccharides, dicarboxylic acids and tricarboxylic acids [21]. The type species of the genus *Acidiphilium cryptum* is often found in close association with acidophilic chemoautotrophs such as *At. ferrooxidans*. The syntrophic relationship of the acidophilic species involves organic substances that derive from the autotroph (as exudates or cell lysates) being used as carbon and energy sources by *Acidiphilium* spp., and other heterotrophic acidophiles [21, 22]. Ferric iron generated by iron-oxidizing acidithiobacilli can be used by *Acidiphilium* as an alternative electron acceptor to oxygen in oxygen-limited environments [19]. In addition, carbon dioxide generated by heterotrophic bacteria has been postulated to be used by autotrophic iron- and sulfur-oxidizing acidophiles [23], though this has not hitherto been proven.

Commonly carbon uptake and exchange within microbial consortia is detected by nucleotide-, fatty acid-SIP or by tracing ^{14}C-carbon [24, 25]. In addition, methods such as Raman spectroscopy, microautoradiography, and nanoSIMS have been used to analyze the ^{12}C/^{13}C carbon composition of cell compartments revealing a high resolution of single cells within complex communities [26, 27]. Besides the utmost level of sensitivity, a direct combination of isotope detection and phylogenetic origin is only possible by the concomitant use of phylogenetic probes and microscopy (FISH).

In this study, we used protein-SIP for tracking the carbon flux in a mixed culture of *At. ferrooxidans* and *A. cryptum*. A time-series experiment was set up using ^{13}C-labeled galactose as substrate for *A. cryptum*. *At. ferrooxidans* is a strict chemoautotroph [21] and is not able to catabolize galactose or other monosaccharides. In a hypothetical model, a release of $^{13}CO_2$ by the heterotrophic species is assumed, which then is assimilated by the autotrophic species. In the course of the metabolic activity, ^{13}C-labeled organic exudates are formed which might be used again by the heterotroph. The quantification of time-dependent ^{13}C incorporation into the proteins of *At. ferrooxidans* and *A. cryptum* was measured by mass spectrometric analysis. The results from this study of a simple microbial community can be used to estimate the generic applicability of the protein-SIP method for carbon flux analysis.

2. Materials and methods

2.1 *Bacterial strains and growth conditions*

A. cryptum^{T} (DSM-2389) and *At. ferrooxidans*^{T} (DSM-14882) obtained from the German Collection of Microorganisms and Cell Cultures (DSMZ; Braunschweig, Germany) were used in the experimental work. *A. cryptum* was grown in a medium containing basal salts and trace elements (pH 3.0) [28] supplemented with 10 mM galactose, at 30°C and with continuous shaking (130 rpm). *At. ferrooxidans* was pre-cultured under the same growth conditions but the growth medium was supplemented with 2.5 mM potassium tetrathionate instead of galactose.

2.2 *Experimental set up and sampling*

Pure cultures of *At. ferrooxidans* and *A. cryptum*, grown as described above, were harvested in early stationary growth phase by centrifugation (11,000 x g, 30 min, 4°C) in an AvantiTM J-30I centrifuge (Beckman Coulter, Fullerton / USA). Cell pellets were washed several times with basal salts (pH 3.0) to remove any remaining traces of galactose or tetrathionate. Pellets were resuspended in basal salts pH 3.0 and cell numbers were determined using a Thoma counting chamber.

For the main experiment, 15 identical cultures were set up in 250 ml shake flasks, each containing 60 ml of growth medium (basal salts/trace elements, supplemented with 2.5 mM potassium tetrathionate and 1 mM ^{13}C galactose (Campro Scientific, The Netherlands) at pH 3.0). Five additional shake flasks containing unlabeled galactose (and tetrathionate) were set up as controls. Cells from the pre-cultures of *At. ferrooxidans* and *A. cryptum* were inoculated into fresh media, giving a final cell number of $2*10^3$ cells/ml of each bacterium. The shake flasks were closed air-tight using screw-tops with central rubber septa, to allow sampling of the gas and liquid phases. The flasks were incubated in a rotary shaker (130 rpm) at 30°C. Control flasks were sampled on a daily basis to determine concentrations of galactose and tetrathionate and to measure pH. At different points in the culture growth cycles, triplicate flasks containing ^{13}C galactose and one control flask were removed. Eight milliliters of the gas phase were removed from each flask using a syringe, and stored in 10 ml headspace vials (previously flushed with nitrogen). Next, the flasks were opened and 5 ml aliquots of the liquid phase were withdrawn for FISH analysis

(described below) and the cells in the remaining liquid phase were concentrated by centrifugation (11,000 x g, 30 mins, 4° C). The supernatant and the cell pellet were stored separately at -20°C for further analysis. A small volume of the supernatant was also used for final determination of pH and concentrations of galactose and tetrathionate.

2.3 *Physicochemical analysis*

The pH in the liquid phase was determined using a combined Sentix20 pH electrode (WTW, Germany) coupled to a Calimatic 766 pH meter (Knick, Germany). Tetrathionate was assayed by cyanolysis as described by Kelly et al. [29]. Galactose was determined as previously described [10].

2.4 *Fluorescent in situ hybridization (FISH)*

Five milliliters of each sample were concentrated by centrifugation for 15 min at 11,000 × g and 4°C. Cell pellets were suspended in 100 µl of the residual fluid and fixed by adding three volumes of a paraformaldehyde solution (4% (w/v) in phosphate-buffered saline (PBS)). After fixation for 3 h at 4°C, cells were washed in 1×PBS and stored in ethanol:1×PBS (1:1) at −20°C until analyzed [30, 31]. To determine total cell numbers, cells present in the samples were stained with 4-,6-diamidino-2-phenylindole (DAPI) and visualized by epifluorescence microscopy. Enumeration of the DAPI-stained cells was performed on Teflon-coated glass by using 2 µl of the fixed cell suspension. For hybridization of *At. ferrooxidans* cells the oligonucleotide probe used was TF539 (5'- CAG ACC TAA CGT ACC GCC -3') labeled with fluorescein at the 5'-end, according to [32], while for *A. cryptum* the probe used was Acdp821 (5'- AGC ACC CCA ACA TCC AGC ACA CAT -3') Cy3-labeled at the 5' end, as described in [33].

To adjust the probe specificity, the hybridization buffer for TF539 was supplemented with 20% (v/v) formamide and for Acdp821 with 25% (v/v) formamide. Hybridization was performed at 46°C and washing at 48°C for both probes. Washing solutions were prepared as described previously [34].

2.5 *Protein extraction*

Cell pellets were suspended in 200 µl of urea buffer (8 M urea, 40 mM Tris-HCl pH 7.5, 4 mM DTT, 1 mM PMSF, 1 µl/ml benzonase) and subsequently disrupted by three cycles of ultrasonic treatment under continuous cooling on ice (ultrasonic processor UP50H equipped with ultrasonic probe MS1, Hielscher ultrasonics, Teltow, Germany). After incubation for 1.5 h at room temperature, cell debris were separated by centrifugation at 16,000 x g for 20 min and 4°C (Laboratory Centrifuge 3K30, Sigma, Osterode, Germany). The supernatant was kept at 4°C and immediately subjected to further processing steps.

2.6 *Protein separation and mass spectrometric analysis*

Protein concentration was determined using the Bradford assay [35].{Marion M, 1976 #972} For 1-dimensional gel electrophoresis (1-DE), 50 µg of protein were precipitated with five-fold volume of ice-cold acetone and separated using a 12% acrylamide separating gel and the Laemmli-buffer system. After electrophoresis, protein bands were stained by colloidal Coomassie Brilliant Blue G-250 (Roth, Kassel, Germany). One protein band in the mass range of 55 – 65 kDa was cut and subsequently in-gel tryptic digestion was performed [3]. Tryptic peptides of each band were desalted by C_{18} ZipTip columns before MS-analysis.

Peptides were analyzed by UPLC-LTQ Orbitrap-MS/MS as described in Bastida *et al.* [11]. The peptides of the ^{12}C sample and the first ^{13}C replicate were eluted over 16 min with 2–80% solvent B (acetonitrile + 0.1% formic acid) gradient using a nanoAcquity UPLC column (C18, 75 mmx15 cm, 1.75 mm, Waters). Continuous scanning of eluted peptide ions was carried out between 400-2,000 *m/z*, automatically switching to MS/MS CID mode on ions exceeding an intensity of 3000. Raw data were processed for database search using Thermo® Proteome Discoverer software (v1.0 build 43, Thermo Fisher Scientific). Search was performed by tandem mass spectrometry ion search algorithms from the Mascot house server (v2.2.1). The following parameters were selected: TaxID 524 (*A. cryptum*) and 920 (*At. ferrooxidans*) of NCBInr (National Center for Biotechnology Information, Rockville Pike, USA, version August 2010 and later) as criterion for taxonomy, tryptic cleavage, maximal two missed cleavage sites. A peptide tolerance threshold of ±10 ppm and an MS/MS tolerance threshold of ±0.2 Da were chosen. Carbamidomethylation at cysteines was given as static and oxidation of methionines as variable modification. Only proteins with at least 2 identified peptides with a false-positive probability less than 0.05 (ion score threshold >40) were considered for further analysis.

2.7 *Calculation of relative isotope abundance (RIA) and labeling ratio (lr)*

Mass spectra were analyzed as described previously [8, 10]. In brief, the spectra were analyzed manually using QualBrowser v2.0.7 (Xcalibur®, Thermo Fisher Scientific Inc., Waltham MA, USA). The percentage of incorporated ^{13}C atoms in relation to the total number of carbon atoms in a peptide (RIA) was calculated by a widely applied method based on comparison of theoretical and experimental spectral data. For semi-automatic calculation of the RIA, an Excel spreadsheet was used as described in Taubert et al. [8] (downloadable from the Helmholtz Centre for Environmental Research – UFZ, Department of Proteomics: http://www.ufz.de/index.php?en=20647).

The labeling ratio defined by Taubert et al. [8] as the proportion of a peptide's heavy isotope-labeled isotopologues of all isotopologues of that peptide, thereby having a range between 0 (only unlabeled peptide) and 1 (only labeled peptide), was calculated to compare the labeled and unlabeled

peptide abundances in any one sample.

The workflow for the calculation was similar to that described by Taubert et al. [8]: *(i)* a mass range covering the masses of heavy and light isotopologues of a peptide was selected and (*ii*) the peak intensities of both light and heavy isotopologues were compared within a sample using a timeframe adjusted to the elution time of the peptide to calculate the labeling ratio.

$$\text{labeling ratio} = \frac{\sum(\text{intensities of isotope peaks of specific incorporation pattern})}{\sum(\text{intensities of all isotope peaks of the peptide})}$$

If more than one incorporation pattern was detected, labeling ratios had to be calculated for all patterns individually. For calculation of the labeling ratios on protein level, data of at least three peptides were averaged.

3. Results and discussion

3.1 *Cultivation*

At. ferrooxidans and *A. cryptum* were grown as a mixed culture containing both ^{13}C-labeled galactose and non-labeled tetrathionate, together with control cultures containing non-labeled galactose and tetrathionate. Microbial growth was monitored by measurement of pH, tetrathionate and galactose (Figure 1A). Tetrathionate originally present in the culture medium (2.3 mM) was completely oxidized (by *At. ferrooxidans*) after 10 days of incubation. Additional tetrathionate (2.3 mM) was added on day 16, which was oxidized within two days due to greater numbers of *At. ferrooxidans* being present by this time. The metabolic activity of *A. cryptum* was confirmed by the fact that all of the galactose in the medium had been removed by day 8. Although recent genome analysis of the type strain of *At. ferrooxidans* has identified a galactose proton symporter-like gene, this has been suggested to be involved in molecular signaling [36]. Cultivation experiments of *At. ferrooxidans* showed that the species does not catabolize galactose. The pH of the medium changed from 3.0 to 1.87 during the incubation period, due to oxidation of tetrathionate to sulfuric acid.

Growth of the two acidophiles was confirmed by cell counts using FISH probes specific for each of the two species. Cell numbers of *A. cryptum* (Figure 1B) increased from ~ $2.0*10^3$ to $1.0*10^7$ cells/ml, and those of *At. ferrooxidans* (Figure 1C) from ~ $1.5*10^3$ to $2.5*10^7$ cells/ml over the time course (18 days) of the experiment. Time-related changes in cell numbers were uneven, though this was a consequence of the experimental design which did not track individual cultures but instead involved the harvesting of entire liquid cultures at each time point. The apparent discrepancies were due to these cultures not being perfectly synchronized.

3.2 *Protein identification*

Protein extracts from each time point and replicate were separated via 1-DE, and a gel band covering the protein mass of 55 – 65 kDa was typically digested and further analyzed by mass spectrometry. A total of 104 proteins were identified in the combined searches from all non-labeled substrate cultures (see Table S1). This relatively low number can be explained by the measurement of the defined mass range and

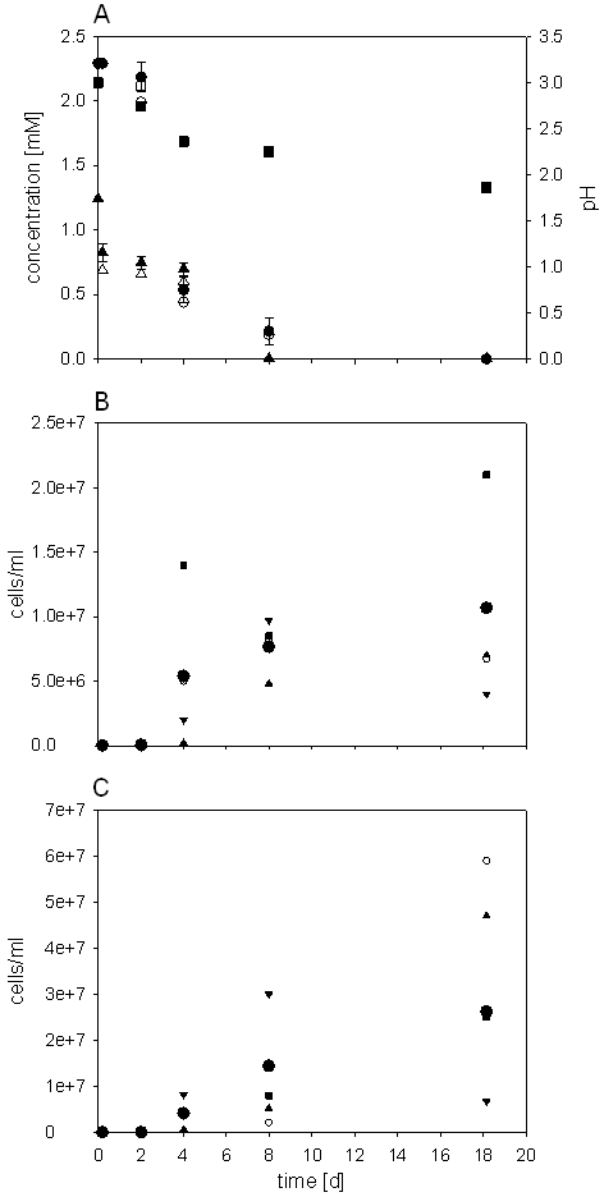

Figure 1. Time course of growth parameters during ^{12}C and ^{13}C cultivations. The upper plot (A) shows galactose concentration of ^{12}C (Δ) and ^{13}C cultures (▲), tetrathionate concentration of ^{12}C (○) and ^{13}C cultures (●), pH of ^{12}C (□) and ^{13}C cultures (■). Values for ^{13}C cultures are given as means of three replicates and corresponding standard deviations. Middle and bottom plots display changes in cell numbers of (B) *A. cryptum* and (C) *At. ferrooxidans* during the experiment. Each plot shows cell numbers in the ^{12}C culture (○) and in three replicates of ^{13}C cultures (replicate one (▲), two (▼), three (■) and average over all replicates (●). Additional tetrathionate (2.3 mM) was added on day 16.

cell numbers being quite low, especially for the first time points.

3.3 *Incorporation of ^{13}C in proteins of A. cryptum*

The RIAs and the lr of peptides from three proteins of the heterotroph *A. cryptum* (chaperonin GroEL, dihydroxy-acid dehydratase and 30S ribosomal protein S1; Table 1) were calculated using the semi-automatic script described by Taubert et al. [8]. The peptides were found to show two distinct incorporation patterns caused by differential incorporation of ^{13}C. As an example, the mass spectral incorporation patterns for peptide AGGLPAVIGELIR of dihydroxy-acid dehydratase at all time points are shown in Figure 2A. An overview of the averaged values from all peptides is given in Figure 3. The pattern showed a rapid appearance of the ^{13}C

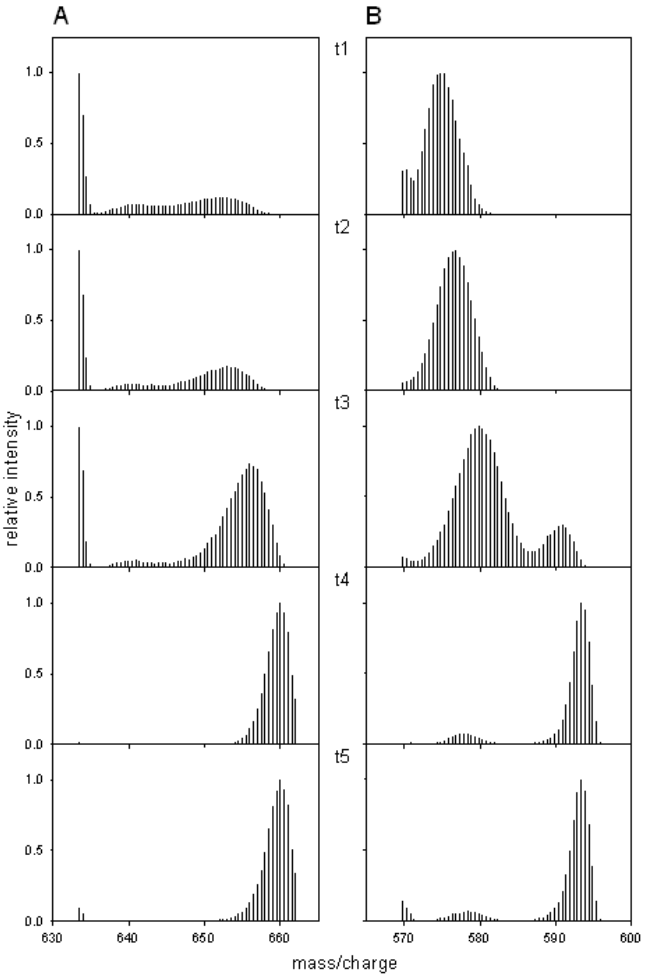

Figure 2. Changes of peptide ion mass distributions during cultivation of *A. cryptum* and *At. ferrooxidans* in mixed culture. Representative mass spectra showing the peptide ion mass distribution of (A) peptide AGGLPAVIGELIR of dihydroxy-acid dehydratase (*A. cryptum*, gi148259108) and (B) peptide AFDGSSIAGWK of glutamine synthetase, type I (*At. ferrooxidans*, gi198282766). Intensity values are given as relative intensity of highest peak in the section depicted.

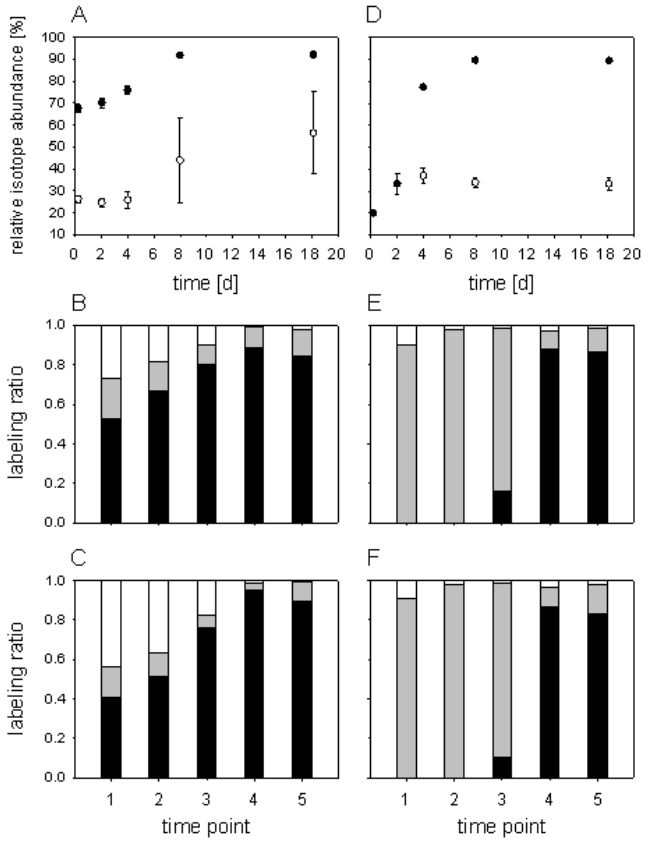

Figure 3. Development of relative isotope abundance (RIA) and labeling ratio (lr) over time in proteins of *A. cryptum* (left side) and *At. ferrooxidans* (right side). In the upper section the time courses of the RIA for (A) *A. cryptum* and (D) *At. ferrooxidans* are shown. In both cases a higher (●) and a lower RIA (○) was detected. Plots are shown as mean values of three replicates, and are based on three proteins in the case of *A. cryptum* (chaperonin GroEL, gi148261486, dihydroxy-acid dehydratase, gi148259108, 30S ribosomal protein, gi148259766) and two proteins in the case of *At. ferrooxidans* (glutamine synthetase type I, gi198282766, chaperonin GroEL, gi198282835). RIA calculations are based on at least three peptides per protein, time point and replicate.
The middle and lower section shows the development of the lr over time in proteins of *A. cryptum* (B and C) and *At. ferrooxidans* (E and F). Bars represent the distribution of the labeling ratios of ^{12}C peak (white), lower ^{13}C RIA peak (grey) and higher ^{13}C RIA peak (black) at each time point of cultivation. *A. cryptum* proteins shown are (B) 30S ribosomal protein S1, gi148259766 and (C) dihydroxy-acid dehydratase, gi148259108. *At. ferrooxidans* proteins shown are (E) glutamine synthetase type I, gi198282766 and (F) chaperonin GroEL, gi198282835. Calculations of lr are based on at least three peptides per protein, time point and replicate. Bars are averaged over three replicates.

isotopologues at time point one (within 5 hours of incubation), exceeding the intensity of the ^{12}C isotopologues at day 8. The first pattern, with an average RIA of around 25% ^{13}C, decreased in relative intensity over time, from a lr of 0.19 ± 0.03 after 5 h of incubation to a final lr of 0.07 ± 0.06 at day 18. Due to the low intensity and the associated difficulties in detection of the pattern in the spectra, both RIA and lr val-

Table 1. List of proteins (gi numbers, organisms, analysed peptides) and the respective calculated RIA and lr values for cultivation on ^{13}C-galactose for the time range 0.2 d to 18 d. Calculations for each protein were averaged for three replicate cultures.

GI no.	Protein name (peptides)	Time [d]									
		0.2		2		4		8		18	
		RIA [%]	lr	RIA [%]	lr	RIA [%]	lr	RIA [%]	lr	RIA [%]	lr
Acidithiobacillus ferrooxidans ATCC 53993											
gi198282766	glutamine synthetase, type I	19.8 ± 0.2	0.90 ± 0.02	32.7 ± 4.8	0.98 ± 0.01	36.4 ± 3.8	0.82 ± 0.04	89.6 ± 0.1	0.88 ± 0.02	89.4 ± 0.4	0.87 ± 0.02
	(AFDGSSIAGWK, LVPHFEAPVLLAYSAK,					77.5 ± 2.0	0.16 ± 0.05	33.0 ± 2.0	0.12 ± 0.02	32.8 ± 3.6	0.12 ± 0.02
	GGYFPVPPVDSAQDLR, AINALTNPSTNSYK)										
gi198282835	chaperonin GroEL	19.8 ± 0.3	0.91 ± 0.02	33.6 ± 4.7	0.98 ± 0.01	37.3 ± 3.7	0.88 ± 0.04	89.5 ± 0.2	0.84 ± 0.03	89.2 ± 0.5	0.84 ± 0.03
	(EVAQVGTISANSDDSIGK,					77.1 ± 0.9	0.11 ± 0.04	34.5 ± 2.5	0.15 ± 0.04	33.5 ± 2.7	0.14 ± 0.04
	EVASQASDEAGDGTTTATVLAQAIIR, LESTTLADLGQAK, TANHDQDmGVAIIR, VVSEEIGmKLESTTLADLGQAK)										
Average *Acidithiobacillus ferrooxidans* proteins		19.8 ± 0.2	0.90 ± 0.02	33.2 ± 4.6	0.98 ± 0.01	36.9 ± 3.7	0.85 ± 0.05	89.5 ± 0.1	0.86 ± 0.03	89.3 ± 0.4	0.85 ± 0.03
						77.3 ± 1.5	0.14 ± 0.05	33.7 ± 2.3	0.13 ± 0.03	33.2 ± 3.1	0.13 ± 0.03
Acidiphilium cryptum JF-5											
gi148261486	chaperonin GroEL	68.3 ± 0.5	0.41 ± 0.02	70.6 ± 1.0	0.57 ± 0.03	74.3 ± 1.7	0.71 ± 0.04	91.3 ± 0.7	0.94 ± 0.09	91.5 ± 1.2	0.94 ± 0.04
	(ITTPSETAQVGTISANGEAEIGK, TNDLAGDGTTTATVLAQAIVR, QIAENAGEDGAVISGK, VGGASETEVKER, GIQTELDVVEGmQFDR, LAGGVAVIR)	25.6 ± 0.8	0.21 ± 0.03	24.0 ± 1.2	0.16 ± 0.03	24.4 ± 2.1	0.10 ± 0.02	43.6 ± 20.2	0.06 ± 0.08	49.4 ± 20.7	0.04 ± 0.04
gi148259108	dihydroxy-acid dehydratase	65.8 ± 2.2	0.41 ± 0.03	69.2 ± 1.9	0.51 ± 0.04	76.3 ± 1.9	0.77 ± 0.05	91.5 ± 0.5	0.97 ± 0.06	91.7 ± 0.1	0.96 ± 0.05
	(QSGTSGSPSILNASPESAVGGGLALLK, FTGQLETGAVLENAPQYQR, STQWFDNPDNPGmTALYLER, IGYEIPLLVNmmPAGK, SANILIDEADLAAR, AG-GLPAVIGELIR)	26.7 ± 1.7	0.16 ± 0.02	24.9 ± 2.1	0.12 ± 0.03	27.1 ± 5.7	0.06 ± 0.02	47.2 ± 21.7	0.04 ± 0.03	69.1 ± 2.9	0.11 ± 0.01
gi148259766	30S ribosomal protein S1	68.1 ± 2.3	0.53 ± 0.05	70.1 ± 3.2	0.67 ± 0.04	77.0 ± 1.5	0.80 ± 0.04	91.6 ± 0.6	0.97 ± 0.06	92.2 ± 1.2	0.93 ± 0.07
	(VLDVDVEKER, DVTPLmGVQQPFQILK, QLETD-PWEGVDVK, SGDTFDLYIER,	25.7 ± 1.3	0.20 ± 0.02	25.0 ± 2.2	0.15 ± 0.02	26.4 ± 4.1	0.10 ± 0.04	34.2 ± 0.1	0.12 ± 0.10	67.1 ± 3.0	0.15 ± 0.04
	SQGADHTTGTEDFAALLDSTLGSNTGFEGSVVSGR, VDDVLTGFIR)										
Average *Acidiphilium cryptum* proteins		67.4 ± 2.0	0.45 ± 0.07	70.0 ± 2.2	0.58 ± 0.07	75.8 ± 2.0	0.76 ± 0.06	91.5 ± 0.6	0.96 ± 0.07	91.8 ± 1.0	0.94 ± 0.06
		26.0 ± 1.3	0.19 ± 0.03	24.6 ± 1.9	0.14 ± 0.03	25.8 ± 4.0	0.09 ± 0.03	43.8 ± 19.1	0.06 ± 0.07	56.2 ± 18.7	0.07 ± 0.06

ues for the later time points showed considerable variations.

The second pattern, with a RIA of 67.4 ± 2.0% ^{13}C after 5 hours and 91.8 ± 1.0 % ^{13}C at day 18, showed a strong increase of the lr from 0.45 ± 0.07 to 0.94 ± 0.06, with the highest increase in intensity between day 4 and 8 (Figure 2A). This represents a high synthesis rate of proteins from a highly ^{13}C-labeled carbon source, and thus a rapid increase in microbial growth [8], which was also apparent from increasing cell numbers (Figure 1B). Within the present experimental setup, this was clearly a result of the metabolism of ^{13}C-galactose. The deviation between the galactose RIA of >=98% and the peptide RIA of 67 to 92% can be explained by the assimilation of unlabeled carbon sources, internal carbon reserves or secreted metabolites of *At. ferrooxidans*. As the first pattern at lower RIA did not show any increase over time, it can be assumed that it was a result of metabolic processes proceeding prior to the first sampling time.

3.4 *Incorporation of ^{13}C in proteins of At. ferrooxidans*

For the autotroph *At. ferrooxidans*, values for RIA and lr of peptides from two proteins (glutamine synthetase, type I and chaperonin GroEL; table 1) were calculated. As an example, the mass spectral incorporation patterns for peptide AFDGSSIAGWK of glutamine synthetase, type I at all time points are shown in Figure 2B. An overview of the averaged values from all peptides is given in Figure 3. As with *A. cryptum,* the ^{13}C isotopologues pattern appeared immediately but the ^{12}C isotopologues showed a low intensity compared to the ^{13}C pattern. An incorporation pattern of around 20% RIA was visible at early time points (Figure 2B). This pattern is increasing in intensity up to day 4, and also a slight increase of the RIA to around 37% can be seen. From this time point on, no further increase in intensity was detected. This development of the pattern can be explained by an oxidation of galactose by *A. cryptum*, and the resulting $^{13}CO_2$ being assimilated by the autotroph *At. ferrooxidans*. Until day 4 the predominant RIA pattern showed rather low ^{13}C-incorporation at a simultaneously high lr indicating the use of ^{13}C-labeled and non-labeled CO_2 (Figure 2B). In addition, another pattern at higher RIA of ~77% appeared at the same time (day 4), which increased to ~ 89% on day 18, also strongly increasing in intensity. This increase of the RIA correlated with the highest metabolic activity of *A. cryptum* as illustrated by the strongly increasing lr between day 4 and 8 (Figure 2). The RIA in the CO_2 fraction would have been expected to increase significantly between day 4 and day 8, due to the oxidation of ^{13}C galactose to $^{13}CO_2$ by *A. cryptum*. Consequently, the shift of the incorporation pattern in *At. ferrooxidans* peptides can be explained by autotrophic CO_2 fixation and the increase of $^{13}CO_2$ produced by *A. cryptum*.

3.5 *Carbon flux analysis*

As the syntrophic interaction between *A. cryptum* and *At. ferrooxidans* under the present experimental conditions was based on the oxidation of ^{13}C-galactose to $^{13}CO_2$ and the subsequent uptake of labeled CO_2, an increase of the labeling ratio of peptides from *A. cryptum* should correlate with an increase of the RIA of peptides from *At. ferrooxidans*. After a certain time, while a sufficient amount of $^{13}CO_2$ is produced by the heterotroph and assimilated by the autotroph, a similar RIA value should also have been detected in peptides of the autotroph. With the data obtained, both effects were observed. After an initial lag phase, *A. cryptum* displayed maximal protein biosynthesis rate (growth) between day 4 and day 8, as illustrated by both significantly increasing lr and cell numbers. Besides the use of ^{13}C-labeled galactose, the RIA development of *A. cryptum* can be caused by the additional uptake of organic exudates and lysates from *At. ferrooxidans*, and the use of internal ^{12}C carbon reserves which are depleted after day 4. In addition, the increased value of the RIA at the last two time points could be explained by increased ^{13}C-incorporation in organic exudates and lysates as a result of increasing uptake of $^{13}CO_2$ by *At. ferrooxidans*. $^{13}CO_2$ formation was detected by GC-C-IRMS measurements (data not shown). The overall syntrophic interaction between both species is shown in Figure 4.

Heterotrophic acidophilic microorganisms such as *Acidiphilium* spp. have often been found living in association with acidophilic chemolithoautotrophs such as *At. ferrooxidans* [37]. This partnership has been reported for several microbial communities in natural acidic habitats (e.g. the Tinto river), acid mine drainage and "biomining" environments [22, 38]. The heterotrophs are capable of using at least some of the organic compounds secreted by the autotrophs and, by removing these, help to maintain conditions that are conducive to the growth of the autotrophs. This is particularly important in closed environments (e.g. stirred tanks used for mineral bioprocessing) where concentrations of some soluble carbon exudates might otherwise inhibit the growth and activities of chemoautotrophic bacteria [23]. Liu et al. recently found that in an artificial mixed culture of *A. acidoph-*

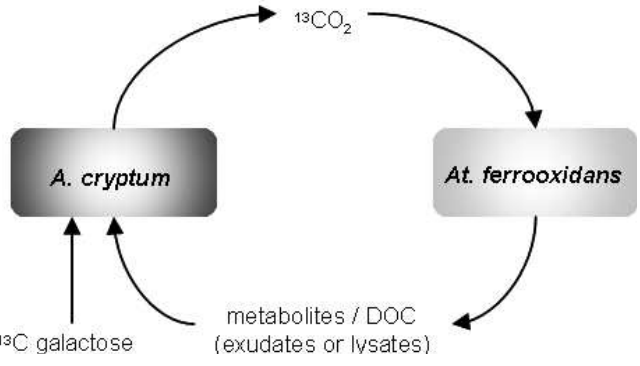

Figure 4. Carbon flow within the syntrophic interaction of *A. cryptum* and *At. ferrooxidans*. The heterotroph catabolized ^{13}C labeled galactose and released $^{13}CO_2$ which was taken up and assimilated by the autotroph. In course of its metabolism the autotroph secreted dissolved organic compounds (DOC) which in turn were metabolized by the heterotroph.

ilum and *At. ferrooxidans* growth of the autotroph was promoted by the heterotrophic partner by activating genes related to iron oxidation and CO_2 fixation [39]. The ability of heterotrophic acidophiles to remove inhibitory organic compounds and thereby facilitate the growth of iron- and sulfur-oxidizing acidophiles is also the basis of the "overlay" plate technique for cultivating the latter on solid media, though here the organic materials are thought mostly to derive from the acid hydrolysis of the gelling agent (agar and derivatives) [40]. The "feedback" mechanism where carbon dioxide released by the heterotrophs is used by the autotrophs has previously been alluded to [23] but had not been proven. Data from the current work has confirmed that this does indeed occur.

4. Concluding remarks

The applicability of protein-SIP to track carbon transfers in a defined mixed culture of autotrophic and heterotrophic bacteria was successfully demonstrated. Two-way transfer of carbon was confirmed by changes of mass spectral patterns. Protein-SIP is therefore a potential technique for examining more complex microbial communities where metabolic activities of microbial key players can be detected and quantitatively described. In addition, secondary consumers using metabolites from the primary species and putative scavengers are detectable by protein-SIP, allowing the construction of a carbon-based food web of a microbial community. Besides the relatively high amount of biomass needed and the dependency of appropriate genomic data, Protein-SIP has some major advantages compared to other SIP approaches: *i)* DNA/RNA-SIP has a 100 fold lower accuracy and sensitivity, and no conclusion of a direct or indirect metabolisation of the carbon source can be achieved; *ii)* PLFA-SIP has a low phylogenetic resolution and a concomitant detection of differentially labeled phospholipid fatty acids is not possible. The progress in bioinformatics tools allowing an automatic analysis will increase the potential of protein-SIP for complex studies.

5. Supplementary material

Supplementary data and information is available at: http://www.jiomics.com/index.php/jio/rt/suppFiles/85/0

Supplementary material includes Fig. S1 showing the pictures of the 1-dimensional (1-DE) SDS gels of the samples. Table S1 includes all proteins identified in the ^{12}C samples.

Acknowledgements

S. Hedrich was funded by a Ph.D. scholarship of the German Federal Environmental Foundation (DBU) and M. Taubert was funded by the Deutsche Forschungsgemeinschaft (SPP 1319). We thank U. Günther for her support with GC-C-IRMS measurements.

References

1. M. G. Dumont, J. C. Murrell, Nat. Rev. Microbiol. 3 (2005) 499-504.
2. N. Jehmlich, F. Schmidt, M. von Bergen, H. H. Richnow, C. Vogt, ISME J. 2 (2008) 1122-1133.
3. N. Jehmlich, F. Schmidt, M. Hartwich, M. von Bergen, H. H. Richnow, C. Vogt, Rapid Commun. Mass Spectrom. 22 (2008) 2889-2897.
4. N. Jehmlich, F. D. Kopinke, S. Lenhard, F. A. Herbst, J. Seifert, U. Lissner, U. Völker, F. Schmidt, M. von Bergen, Proteomics 12 (2012) 37-42.
5. N. Jehmlich, F. Schmidt, M. Taubert, J. Seifert, F. Bastida, M. von Bergen, H. H. Richnow, C. Vogt, Nat. Protoc. 5 (2010) 1957-1966.
6. N. Jehmlich, F. Schmidt, M. Taubert, J. Seifert, M. Von Bergen, H. H. Richnow, C. Vogt, Rapid Commun. Mass Spectrom. 23 (2009) 1871-1878.
7. N. Jehmlich, I. Fetzer, J. Seifert, J. Mattow, C. Vogt, H. Harms, B. Thiede, H. H. Richnow, M. von Bergen, F. Schmidt, Mol. Cell. Proteomics 9 (2010) 1221-1227.
8. M. Taubert, N. Jehmlich, C. Vogt, H. H. Richnow, F. Schmidt, M. von Bergen, J. Seifert, Proteomics 11 (2011) 2265-2274.
9. I. Fetzer, N. Jehmlich, C. Vogt, H. H. Richnow, J. Seifert, H. Harms, M. von Bergen, F. Schmidt, BMC Res. Notes 3 (2010) 178.
10. M. Taubert, S. Baumann, M. von Bergen, J. Seifert, Anal. Bioanal. Chem. 401 (2011) 1975-1982.
11. F. Bastida, M. Rosell, A. G. Franchini, J. Seifert, S. Finsterbusch, N. Jehmlich, S. Jechalke, M. von Bergen, H. H. Richnow, FEMS Microbiol. Ecol. 73 (2010) 370-384.
12. F. Bastida, S. Jechalke, P. Bombach, A. G. Franchini, J. Seifert, M. von Bergen, C. Vogt, H. H. Richnow, FEMS Microbiol. Ecol. 77 (2011) 357-369.
13. A. R. Colmer, K. L. Temple, M. E. Hinkle, J. Bacteriol. 59 (1950) 317-328.
14. E. Drobner, H. Huber, K. O. Stetter, Appl. Environ. Microb. 56 (1990) 2922-2923.
15. A. B. Jensen, C. Webb, Process Biochem. 30 (1995) 225-236.
16. K. B. Hallberg, D. B. Johnson, Adv. Appl. Microbiol. 49 (2001) 37-84.
17. A. Amouric, C. Brochier-Armanet, D. B. Johnson, V. Bonnefoy, K. B. Hallberg, Microbiology 157 (2011) 111-122.
18. S. Hedrich, M. Schlömann, D. B. Johnson, Microbiology 157 (2011) 1551-1564.
19. D. B. Johnson, FEMS Microbiol. Ecol. 27 (1998) 307-317.
20. N. Kishimoto, Y. Kosako, N. Wakao, T. Tano, A. Hiraishi, Syst. Appl. Microbiol. 18 (1995) 85-91.
21. D. B. Johnson, K. B. Hallberg, in: Poole, R. K. (Ed.), Advances in microbial physiology, Academic Press 2009, pp. 201-255.
22. E. Gonzalez-Toril, E. Llobet-Brossa, E. O. Casamayor, R. Amann, R. Amils, Appl. Environ. Microbiol. 69 (2003) 4853-4865.
23. D. E. Rawlings, D. B. Johnson, Microbiology 153 (2007) 315-324.
24. J. D. Neufeld, M. Wagner, J. C. Murrell, ISME J 1 (2007) 103-110.

25. N. Finke, T. M. Hoehler, B. B. Jorgensen, Environ. Microbiol. 9 (2007) 1060-1071.
26. W. E. Huang, K. Stoecker, R. Griffiths, L. Newbold, H. Daims, A. S. Whiteley, M. Wagner, Environ. Microbiol. 9 (2007) 1878-1889.
27. N. Musat, R. Foster, T. Vagner, B. Adam, M. M. M. Kuypers, FEMS Microbiol. Rev. (2011)
28. K. Wakeman, H. Auvinen, D. B. Johnson, Biotechnol. Bioeng. 101 (2008) 739-750.
29. D. P. Kelly, L. A. Chambers, P. A. Trudinger, Anal. Chem. 41 (1969) 898-902.
30. R. I. Amann, W. Ludwig, K. H. Schleifer, Microbiol. Rev. 59 (1995) 143-169.
31. S. J. Giovannoni, E. F. DeLong, G. J. Olsen, N. R. Pace, J. Bacteriol. 170 (1988) 720-726.
32. M. O. Schrenk, K. J. Edwards, R. M. Goodman, R. J. Hamers, J. F. Banfield, Science 279 (1998) 1519-1522.
33. J. Peccia, E. A. Marchand, J. Silverstein, M. Hernandez, Appl. Environ. Microbiol. 66 (2000) 3065-3072.
34. J. Pernthaler, F. O. Glöckner, W. A. Schönhuber, R. Amann, Meth. Microbiol. 30 (2001) 207-226.
35. M. M. Bradford, Anal. Biochem. 72 (1976) 248-254.
36. J. Valdes, I. Pedroso, R. Quatrini, R. J. Dodson, H. Tettelin, R. Blake, 2nd, J. A. Eisen, D. S. Holmes, BMC Genom. 9 (2008) 597.
37. D. B. Johnson, F. F. Roberto, in: Rawlings, D. E. (Ed.), Biomining: theory, microbes and industrial processes., Springer-Verlag/Landes Bioscience, Georgetown, Texas 1997.
38. A. P. Harrison, Jr., Annu. Rev. Microbiol. 38 (1984) 265-292.
39. H. Liu, H. Yin, Y. Dai, Z. Dai, Y. Liu, Q. Li, H. Jiang, X. Liu, Arch. Microbiol. 193 (2011) 857-866.
40. D. B. Johnson, J. Microbiol. Meth. 23 (1995) 205-218.